Acta Acustica united with Acustica
Vol. 100 (2014) 440 – 447

DOI 10.3813/AAA.918724

Analytical Modeling of Electrostatic Transducers in Gases: Behavior of Their Membrane and Sensitivity

Thomas Lavergne[1)], Stéphane Durand[2)], Nicolas Joly[2)], Michel Bruneau[2)]

[1)] Laboratoire National de métrologie et d'Essais (LNE), 29, avenue Roger Hennequin, 78197 Trappes cedex, France

[2)] Laboratoire d'Acoustique de l'Université du Maine, (LAUM - UMR CNRS 6613), Avenue O. Messiaen, 72085 Le Mans cedex 9, France. stephane.durand@univ-lemans.fr

Summary

Electrostatic transducers have been appropriately characterized during the last decades for their common use under standard conditions. But nowadays, their miniaturization (using MEMS processes) and their uses for metrological purposes under non-standard conditions (i.e. in high frequency ranges, in gas mixtures, and at various static pressures and temperatures) require a much deeper characterization with respect to these uses. Though recent literature on this topic [Lavergne et al., J. Acoust. Soc. Am., 128(6), pp. 3459-3477, 2010] leads to satisfying results for electrostatic microphones according to these requirements, the analytical solution given is not always sufficiently precise to interpret phenomena and must be improved to characterize more accurately both the displacement field of the membrane up to high frequencies (100 kHz) and the sensitivity as a function of the frequency. Thus, the aim of the work presented here is to propose improvements to this analytical procedure for receivers (even transmitters) when coupling between membranes, slots, holes and cavities are involved. These analytical improvements are obtained in introducing a more realistic volume velocity distribution to describe the fluid flow at the end of each hole. The improved analytical model relates to that presented previously for electrostatic microphones (and is based on it) in order to compare the last analytical results with both the theoretical ones obtained previously and the experimental ones available.

PACS no. 43.38.Bs, 43.38.Hb, 43.20.Tb

1. Introduction

Electrostatic transducers are devices whose properties (sensitivity, bandwidth and reliability) make them powerful measurement tools. For their common use under standard conditions they have been appropriately characterized during the last decades. But nowadays, their miniaturization (using MEMS processes) and their new uses for metrological purposes under non-standard conditions (i.e. in high frequency ranges, in gas mixtures, and at various static pressures and temperatures) require a much deeper characterization as the one available previously.

An analytical model, presented recently in a paper [1] starting up again with a previous one [2], which describes the behavior of the diaphragm of a particular receiver (the electrostatic one) and provides the sensitivity as a function of the frequency, appears to be a convenient tool to tackle (more particularly) the effect of the holes in the backing electrode on the displacement field of the membrane which, because of that, can be highly non-uniform in the highest frequency range. Being concerned by the use of this analytical approach when low uncertainties on the behavior of acoustic fields generated or measured by these transducers are required up to 100 kHz, accurate theoretical results could be obtained provided that the main geometrical parameters, namely here those characterizing the air gap and the holes in the backing electrode, be accounted for in a more realistic manner than in the previous paper [1]. Note that, beyond the numerical approaches [3, 4], an appropriate analytical modeling to estimate accurately the displacement field and the frequency response of transducers (including MEMS devices and non standard conditions) would be of interest when dealing with, among others, the acoustic centre and/or the free-field correction of condenser microphones [5, 6, 7], the measurements in couplers [8], or the free-field calibration in the highest frequency range (up to 100 kHz for measuring for example shockwaves profiles [9]).

Thus, the aim of the work presented here is to propose improvements to the analytical procedure mentioned above for receivers (even transmitters) when coupling between membranes, slots, holes and cavities are involved. The improved analytical model relates to that presented

Received 28 July 2013,
accepted 28 February 2014.

previously for electrostatic microphones (and is based on it) in order to compare new analytical results with both the theoretical ones obtained previously and the experimental ones available. The improvements are obtained in describing analytically the effect of each hole from an appropriate volume velocity distribution provided by several virtual point sources (sinks) instead of only one monopole source as assumed in the previous paper. Furthermore, results from a pure numerical simulation concerned with examining the behavior of the acoustic velocity fields around the interface between the holes and the air gap are shown. Accordingly, these results help both choosing the set of the equivalent virtual point sources and interpreting the value of the parameters used in the analytical simulations [10] (including an empirical evaluation of the porosity of the backing electrode which may be different from the geometrical porosity because of this velocity profile). Finally, experimental results, obtained using a laser scanning vibrometer, are presented and compared to the analytical ones, showing good agreements between them and the analytical results for both the displacement field of the membrane up to 100 kHz (for a half-inch microphone) and the sensitivity as a function of the frequency. These results show that the analytical procedure used herein to model the phenomena occurring around the holes in the air gap significantly improves results which can be obtained from an analytical approach recently published, and consequently that this kind of modeling could be adapted to other configuration of transducers.

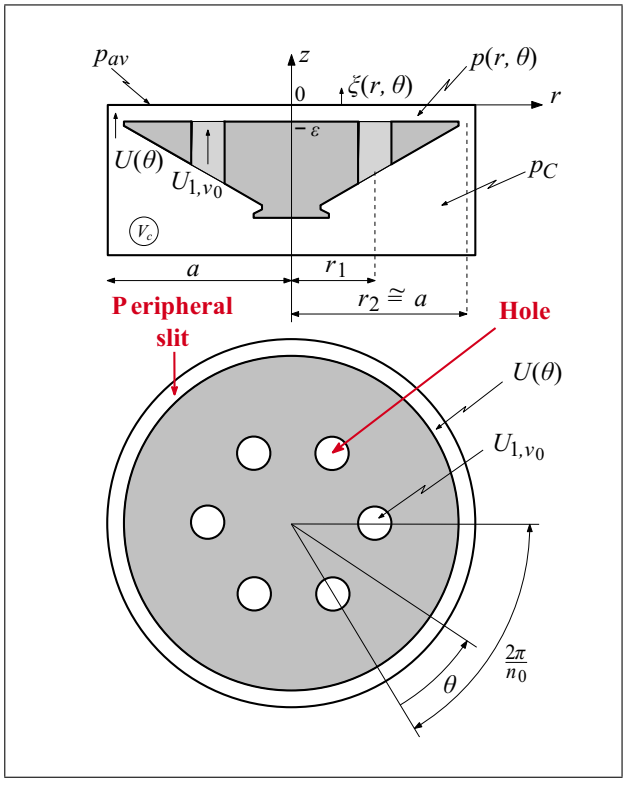

Figure 1. Electrostatic microphone showing the membrane, the backing electrode with holes regularly azimuthally distributed, the peripheral slot, and the backchamber (see notations in the Appendix).

2. The improved analytical approach

The analytical procedure whereby one expresses the behavior of such transducers, which involves coupling between membranes, slots, holes and cavities, was presented in a previous paper [1] and is briefly outlined in the Appendix in its improved form. This analytic procedure relies fundamentally on the coupled differential equations for the fields of each identified domain (membrane, fluid gap, holes, slot, and backchamber shown in Figure 1), then on analytical solutions obtained from both integral formulations and modal analysis. The methodology used in this previous paper to express the boundary conditions and the interface conditions (between domains) are either the classical ones when they are uniform (Dirichlet conditions for the membrane, Neumann conditions around the fluid gap, viscous and thermal impedance-like boundary conditions for the holes, the slot, and the backchamber) or mixed boundary conditions at the interface between the fluid-cavities (gap and backchamber) and the backing electrode (which involve porosity of the electrode and both free and non slip conditions).

In the present paper, the improvements are obtained in considering a more realistic behavior of the acoustic velocity fields around the interface between the holes and the air gap (see Appendix). First, improvements on the shape of the displacement field of the membrane, and consequently on the amplitude of the sensitivity, are obtained in introducing in the calculation a more realistic volume velocity distribution to describe the fluid flow at the end of each hole, instead of representing this end by the virtual point source considered previously (see the right hand side of equations A3, A6, and A7), even though this volume velocity distribution remains reduced to several equivalent volume velocity virtual point sources (the localisation of these sources resulting from a specific numerical calculation).

Second, improvements are also obtained in accounting for an empirical evaluation of the porosity of the backing electrode (defined as the ratio of the total area of the holes to the total backing electrode area) which may be different from the geometrical porosity because of the velocity profile around the sharp edges of the holes. As presented below, these improved calculations, involving the holes mentioned above but also the peripheral slot (in an appropriate manner), give more realistic results for the displacement profiles of the membrane, even when the influence of the holes is predominant, and permit to interpret quantitatively with a very good accuracy the sensitivity curve over the total frequency range of interest (including the resonance frequency). Note that additional losses owing to separation of flow and even formation of vortices which may appear around the sharp ends of the holes and the slot [11] are neglected herein because they are much smaller than the losses in the air gap (approximately three order of magnitude smaller).

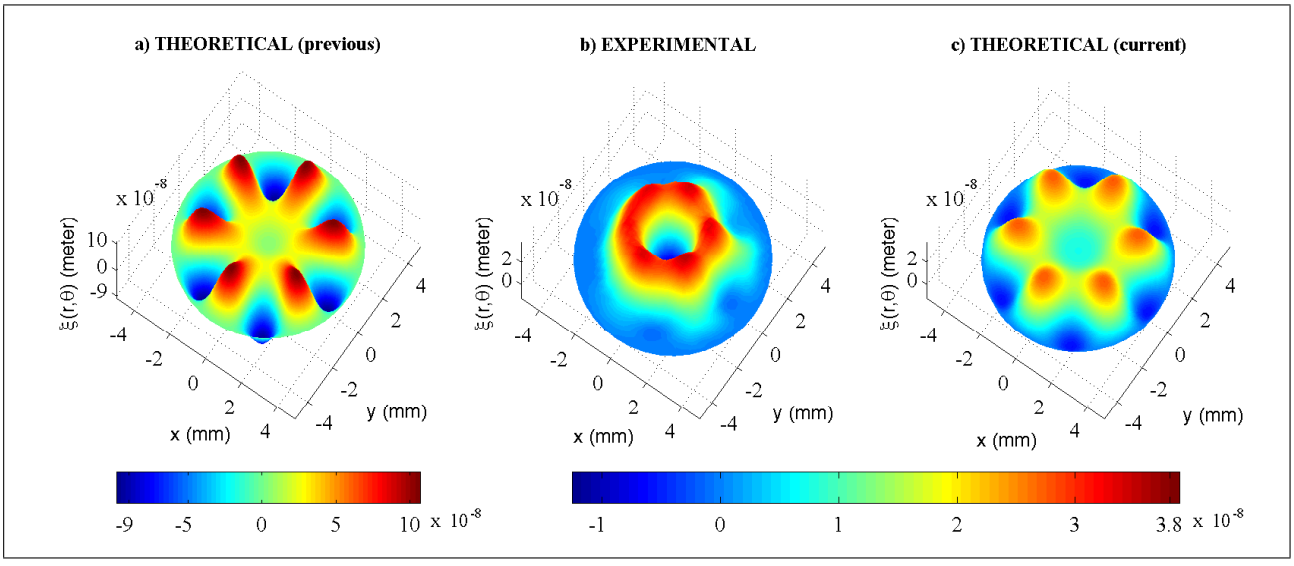

Figure 2. Displacement field of the membrane at 70 kHz. a) Theoretical result obtained from the analytic procedure as it is proposed in the previous paper [1]. b) Experimental result obtained from measurements of the displacement field using a laser scanning vibrometer. c) Theoretical result obtained from the improved analytic procedure as it is proposed herein.

3. Improved analytical results

3.1. Displacement field of the membrane

In each result presented hereafter, the values of the geometrical, mechanical, and electrical parameters are those given in references [1,2] for a half-inch B&K microphone type 4134, except the static capacity, which is herein the one (19.3 pF) occurring when the polarization voltage is applied (given in the calibration charts of the microphones). Figures 2a, 2b, and 2c show, at 70 kHz, respectively the theoretical displacement field of the membrane obtained from the analytic procedure as it is proposed in the previous paper [1], the experimental results obtained from measurements of the displacement field using a laser scanning vibrometer, and the theoretical displacement field obtained from the improved analytic procedure as it is proposed herein (outlined in the Appendix). In both theoretical results, the modes $m = 0$ and $m = 6$ (with $n = 0$ to $n = 15$) are accounted for in order to emphasize the role played by the six holes in the backing electrode.

In the theoretical modeling which gives results shown in Figure 2a, each hole and the peripheral slot are modeled as an equivalent monopole virtual sources localized at their centre (point and linear sinks respectively), as proposed in the previous paper [1]. The consequence of using such simplified model is the significant deviations which appear between the theoretical results and the experimental one (Figure 2b). These deviations (even part of these deviations arises from the error pointed out at the end of the Appendix) are evidence that the approximations assumed in this previous model, although appropriate to describe the intricate behavior of the membrane in the highest frequency range, are too drastic to characterize accurately the behavior of the fluid in the air-gap, and, consequently, the influence of the "sinks" on the displacement field of the membrane. This is particularly true at certain frequencies (here 70 kHz) where the displacement is highly non-uniform.

More accurate analytical results can be obtained by using the alternative model presented herein (see Appendix) which accounts for more realistically the shape of the holes and the slot, as it is evident from the comparison between the analytical results shown in Figure 2c and the experimental results (Figure 2b). In the theoretical modeling which gives results shown in Figure 2c, each hole is modeled as equivalent multipole virtual sources wisely localized (point sinks) and the slot is modeled by a virtual circular line source. Actually these results are not perfect but the amplitude of the maxima are greatly improved (these improvements being not due to the correction of the error in the previous paper mentioned at the end of the present paper).

In order to optimize the number of point sources and the localizations of each source to represent accurately the effect of both the holes and the peripheral slot on the acoustic field in the air-gap, a 2-D axisymmetrical (annular slot centered on the z-axis, Figure 1) numerical simulation using an anisotropic mesh and accounting for the viscous and thermal boundary layer effects [10] has been handled for a uniform displacement field of the membrane. This mapping gives an approximate flow pattern at the interface between holes or slot and air-gap (Figure 3), the arrows representing its direction and the color map the normalized amplitude of its axial component (which is the only relevant component here).

It appears clearly that the main contribution to the strength of the volume velocity of the orifice occurs near the sharp edge (note that at the bottom of Figure 3 the normalized amplitude $v_z/v_{z_{max}}$ is equal to 0.175). Then, it is appropriate to describe each hole by several monopole sources regularly distributed near the sharp edge around the hole instead of a single monopole located in its centre,

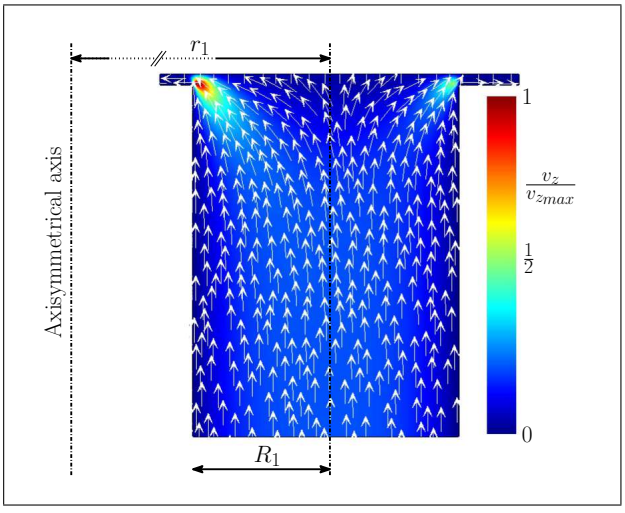

Figure 3. Mapping of the particle velocity field at the interface between holes or slot and air-gap for an approximate axisymmetrical flow. Arrows: direction of the velocity. Color map: normalized amplitude of the axial component of the velocity (at the bottom of the figure, on the axis, the normalized amplitude $v_z/v_{z_{max}}$ is equal to 0.175).

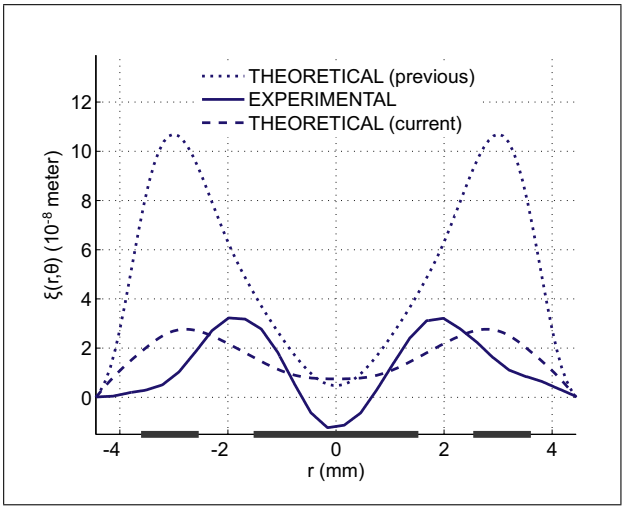

Figure 4. Profiles (along a diameter passing through the center of opposite holes) of the displacement field of the membrane presented in Figure 2. Dotted line: theoretical result obtained from the previous modeling (Figure 2a). Solid line: experimental result (Figure 2b). Dashed line: theoretical result obtained from the modeling considered herein (Figure 2c). The thick interrupted line on the horizontal axis represents a cut of the backing electrode showing the location and diameter of the holes.

and to describe the annular slot by a circular line source near its inner edge. One circular line and four point sources of the same strength are considered in the results presented in Figure 2c (two along the radius of the microphone and two on the same circular line passing through the centre of the hole). The results show that the ability of the analytical method to provide reasonable estimates of both the amplitude of the membrane displacement and to a certain extent the spatial variations is manifest. Note that the mapping in Figure 3 shows that the amplitude of the axial component of the particle velocity is greater on the left side, i.e. toward the centre of the microphone, than on the other side. Then, the velocity sources would be distributed or their strength weighted according to this result, which would better localize the maxima of the displacement field of the membrane. Figure 4 shows the cross-sections (along a diameter passing through the centre of opposite holes) of the displacement field of the membrane presented in Figure 2: theoretical result obtained from the previous modeling (Figure 2a, dotted line), experimental result (Figure 2b, solid line), theoretical result obtained from the modeling considered herein (Figure 2c, dashed line) (the thick interrupted line on the horizontal axis represents a cut of the backing electrode showing the location and diameter of the holes). These results confirm clearly the conclusions above-mentioned. Note that the second resonance frequency of the membrane in vacuo (67.2 kHz) is very closed to the working frequency (70 kHz).

These results enlighten that, given the relative simplicity of the model used herein to describe the behavior of the holes and the slot, there is seen to be close agreement between the experimental results and the analytical results (which improve clearly the analytical results obtained from the previous model). It should also be noted that the uncertainties on the relative strengths or locations of the multipole sources could contribute to the radial shift which appears between theoretical and experimental curves. It should be noted that the uncertainties on the relative strengths or locations of the multipole sources, which are guided herein only qualitatively by the velocity profiles obtained numerically (Figure 3 shows an example of such a profile), could contribute to the radial shift which appears between theoretical and experimental curves.

Figure 5 and Figure 6 provide, at 40 kHz, the same comparison as that presented in Figure 2 and Figure 4 respectively. As expected, these results are consistent with those discussed above.

3.2. Sensitivity of the microphone

Figures 7.a and 7.b show, respectively, the modulus and the phase of the sensitivity of the microphone, defined by the ratio of the open circuit output voltage and the incident pressure (the contribution of the higher order modes $m \neq 0$ vanishes when integrating over the interval $[0, 2\pi]$),

$$\sigma = \frac{-U_0}{\varepsilon \pi a_{bp}^2 p_{av}} \sum_{mn\sigma} \xi_{mn}^{(\sigma)} \int\int_{S_{bp}} \psi_{mn}^{(\sigma)}(r,\theta)\, r\, \mathrm{d}r\, \mathrm{d}\theta,$$

(see notations in [1] and the Appendix), as a function of the frequency, obtained first from the analytical procedure outlined in the Appendix with two assigned values of the porosity Φ_r of the backing electrode (0.04, dashed-dotted line with crosses) and (0.08, dashed line), and the geometrical porosity (0.12, solid line), second from the previous analytical procedure (dotted line), and third from measurements (dashed line with diamonds and dashed-dotted ine with circles), when considering one azimuthal mode $m = 0$ and sixteen radial modes $n = 0$ to $n = 15$ in the calculus.

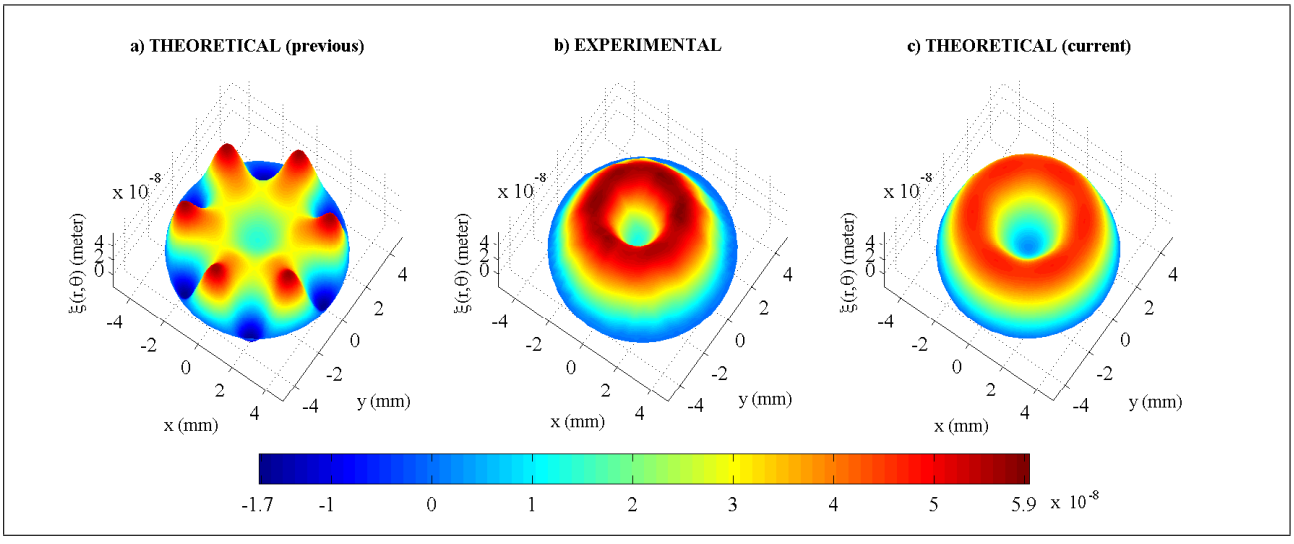

Figure 5. Displacement field of the membrane at 40 kHz. a) Theoretical result obtained from the analytic procedure as it is proposed in the previous paper [1]. b) Experimental result obtained from measurements of the displacement field using a laser scanning vibrometer. c) Theoretical result obtained from the improved analytic procedure as it is proposed herein.

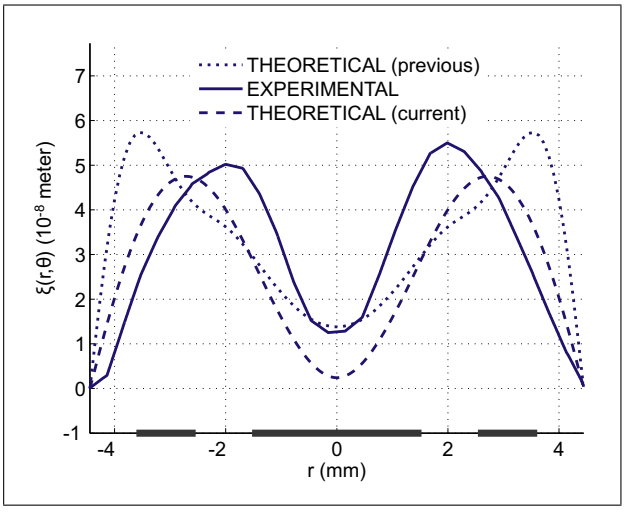

Figure 6. Profiles (along a diameter passing through the centre of opposite holes) of the displacement field of the membrane presented in Figure 5. Dotted line: theoretical result obtained from the previous modeling (Figure 5a). Solid line: experimental result (Figure 5b). Dashed line: theoretical result obtained from the modeling considered herein (Figure 5c). The thick interrupted line on the horizontal axis represents a cut of the backing electrode showing the location and diameter of the holes.

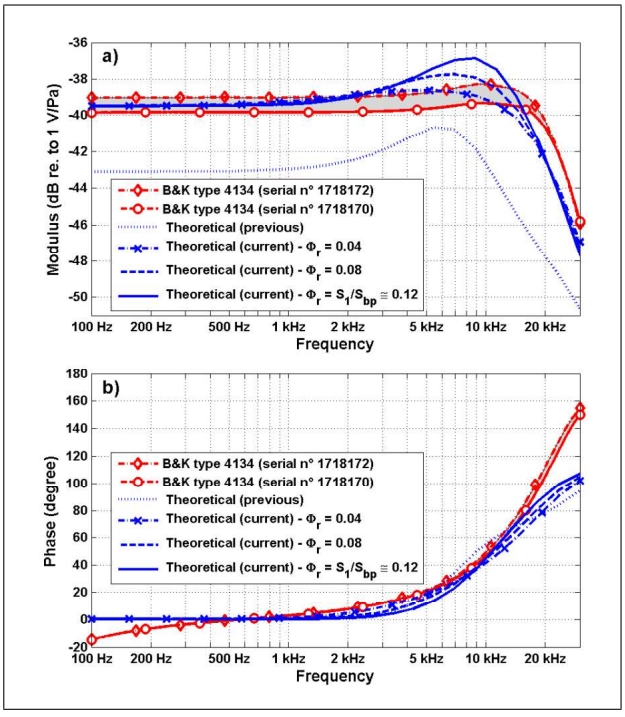

Figure 7. Modulus (a) and phase (b) of the sensitivity as a function of the frequency ($m = 0$ and $n = 0$ to $n = 15$), obtained first from the analytical procedure outlined in the Appendix with two empirical values of the porosity Φ_r of the backing electrode (0.04, dashed-dotted line with crosses) and (0.08, dashed line), and the geometrical porosity (0.12, solid line), second from the previous analytical procedure (dotted line), and third from measurem (dashed line with diamonds and dashed-dotted line with circles).

As expected these results show clearly the relatively good agreement between the analytical results obtained from the improved modeling considered herein and the experimental one (the current analytical results agree better with the experimental results than the previous analytical one), concerning the value of the sensitivity, its resonance frequency, and also its Q-factor when accounting for, through the value of the porosity, the effect of the velocity profile around the interface of the holes or the slot and the fluid gap (Figure 3), and using here (low frequency range, up to 30 kHz) one virtual point source localized on the edge of the holes towards the centre of the electrode and one linear source localized on the edge of the slot.

It should be interesting to relate somewhat these results to the displacement profiles obtained in the frequency

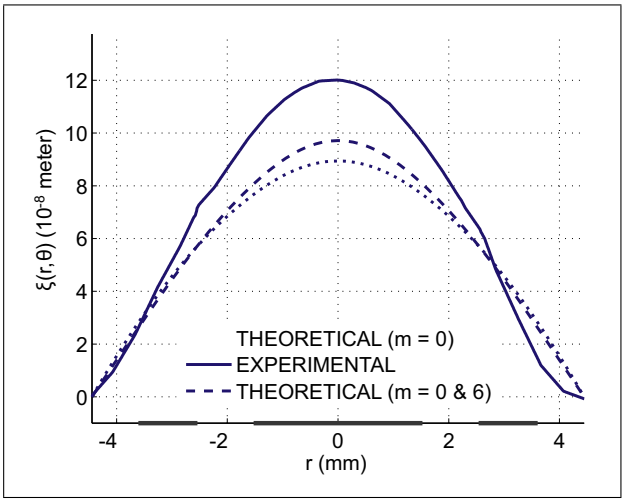

Figure 8. Profils (along a diameter passing through the center of opposite holes) of the displacement field of the membrane at 5 kHz. Dotted line: theoretical result obtained with the current modeling when considering only the azimuthal mode ($m = 0$). Solid line: experimental result. Dashed line: theoretical result obtained with the current modeling considering modes ($m = 0$ & 6). The thick interrupted line on the horizontal axis represents a cut of the backing electrode showing the location and diameter of the holes.

range considered. As an example, Figure 8 provides, at 5 kHz, the comparison of the cross-sections (along a diameter passing through the centre of opposite holes) of the experimental displacement field of the membrane of the B&K microphone #1718172 (solid line) (whose sensitivity is given in Figure 7, dashed-dotted line with diamonds), the displacement fields of the membrane calculated with the current modeling when considering only one azimuthal mode ($m = 0$, dotted line) and when considering two azimuthal modes ($m = 0$ & 6, dashed line) (the thick interrupted line on the horizontal axis represents a cut of the backing electrode showing the location and diameter of the holes). As expected, the theoretical results are close to the experimental one. It is worth noting that the amplitude of the displacement calculated when considering two azimuthal modes is closer to the amplitude of the experimental displacement than when considering only one azimuthal mode. Actually, if the contribution to the sensitivity of the higher order modes ($m \neq 0$) would not vanish, the theoretical sensitivity obtained when considering two azimuthal modes ($m = 0$ & 6) should lead to a closer agreement with the experimental sensitivity. Slight discrepancies remain which could be explained more particularly by the (unknown) uncertainties on the values of the geometrical, mechanical and electrical parameters given in [1] or by the experimental deviations from one microphone to another (dashed-dotted line with diamonds and dashed line with circles). Concerning the behavior of the sensitivity in the vicinity of the resonant frequency, other causes of discrepancies could be mentioned, including the effects of the complex shape of the backing cavity and the heat conducting effects on its walls, the non linear movements around the sharp edges (and so on), which are not accounted for in the present modeling. Note that the discrepancies which appear on figure 7.b (phase curves) in the lower and in the upper frequency ranges are respectively due to the effects of the pressure equalisation vent and the effects on the radiation impedance (of the microphone diaphragm) of the electrostatic actuator used in the measurements [12].

4. Conclusion

The aim of this study was to determine whether parameters adjusted to model the phenomena which occur around the holes in the air gap of electrostatic microphones significantly improve results which can be obtained from an analytical approach recently published. The results gathered are consistent with this hypothesis, the conclusive numerical and experimental results confirming that. Moreover, while the analytical modeling presented herein could appear rather cumbersome, the numerical calculations are in fact very rapid to handle and results convey somewhat interpretations of physical phenomena.

Finally, it is noteworthy that the interest of this modeling extends beyond the electrostatic microphone. Indeed the analytical procedure can be adapted to any transducers (transmitters or receivers) which involve coupling between membranes, thin fluid layers, small cavities, and narrow short tubes and slots. Then, further researches could consider other geometrical parameters and the use of the model in real situations concerning miniaturization and/or metrological applications.

Appendix: analytical formulation [1]

The cylindrical coordinate system used (r, θ, z) has its origin at the center O of the membrane and the Oz-axis is perpendicular to the membrane and outwardly directed as indicated on Figure 1. The holes in the backing electrode are regularly azimuthally distributed at the distance r_1 from the center of the electrode. The origin ($\theta = 0$) of the azimuthal coordinate θ is set at the center of a hole in the backing electrode. The thickness of the fluid film trapped between the membrane and the backing electrode is denoted ε (the coordinate of the upper surface of the backing electrode is "$-\varepsilon$"). It has the same order of magnitude as the thickness of the viscous and thermal boundary layers. The pressure variation depends on the radial coordinate. It is assumed to be constant through the thickness of the fluid gap between the membrane and the backing electrode (it does not depend on the z-coordinate).

The set of equations which governs the displacement field $\xi(r, \theta)$ of the membrane (positive when directed along the z-axis), supported on a rigid circular frame at its periphery $r = a$ (Dirichlet boundary condition), driven by an harmonic acoustic pressure p_{av} assumed to be uniform over the surface of the membrane, and loaded by the pressure field $p(r, \theta)$ in the fluid gap between the membrane

and the backing electrode, can be written as

$$T\left(\partial_{rr}^2+\frac{1}{r}\partial_r+\frac{1}{r^2}\partial_{\theta\theta}^2+K^2\right)\xi(r,\theta) = p_{av}-p(r,\theta), \tag{A1}$$

$$\xi(r=a,\theta)=0, \tag{A2}$$

where $K=\omega\sqrt{M_S/T}$, T and M_s being respectively the tension (per unit of length) of the membrane and its mass per unit area, and ω the angular frequency.

Assuming that each hole and the peripheral slot behave as sources (more exactly as sinks) described by the z-component of their particle velocity (positive when directed along the z-axis) respectively $u_1(r,\theta)$ (for each hole labeled v_0) and $u_2(r,\theta)$ (for the slot), and assuming Neumann boundary condition on the external side of the fluid layer (i.e. at $r\cong a$), the set of equations which governs the pressure field $p(r,\theta)$ inside the fluid gap is given by

$$\left(\partial_{rr}^2+\frac{1}{r}\partial_r+\frac{1}{r^2}\partial_{\theta\theta}^2+\chi^2\right)p(r,\theta) = -\frac{\rho_0\,\omega^2}{F_v}\,\frac{\xi(r,\theta)}{\varepsilon}-\frac{\mathrm{i}\,\omega\,\rho_0}{F_v}\sum_{i=1,2}\frac{u_i(r,\theta)}{\varepsilon}, \tag{A3}$$

$$\partial_r p(r=a,\theta)=0, \tag{A4}$$

where the complex wavenumber χ accounts for the angular frequency ω of the field and the properties of the fluid, namely the compressibility and the density ρ_0 through the adiabatic speed of sound c_0, the heat capacity at constant pressure per unit of mass C_p, the specific heat ratio γ, the shear viscosity coefficient μ, and the thermal conduction coefficient λ_h,

$$\chi^2=\frac{\omega^2}{c_0^2}\,\frac{1+(\gamma-1)\,(1-F_h)}{F_v}, \tag{A5}$$

with $F_v = 1-\dfrac{2-\Phi_r}{2}\,\dfrac{\tan(k_v\varepsilon/2)}{k_v\varepsilon/2}$

and $F_h = 1-\dfrac{2-\Phi_r}{2}\,\dfrac{\tan(k_h\varepsilon/2)}{k_h\varepsilon/2}$,

$k_v = \left[(1-\mathrm{i})/\sqrt{2}\right]\sqrt{\rho_0\omega/\mu}$,

and $k_h = \left[(1-\mathrm{i})/\sqrt{2}\right]\sqrt{\rho_0\omega C_p/\lambda_h}$

being the wavenumbers associated respectively to the viscous (shear) and thermal diffusion processes and Φ_r the porosity of the backing electrode, where the volume velocity of each hole u_{1,v_0} (labelled v_0) is the sum of elementary volume velocities U_{1,v_0v_1} (labelled v_1), the total volume velocity of the surface of the holes per unit volume of the air gap of thickness epsilon being given by

$$\frac{u_1(r,\theta)}{\varepsilon} = \sum_{v_0=1}^{n_0}\frac{u_{1,v_0}(r,\theta)}{\varepsilon} = \sum_{v_0=1}^{n_0}\sum_{v_1}\frac{U_{1,v_0v_1}(r,\theta)}{\varepsilon}\,\frac{1}{r} \cdot\delta(r-r_{v_0v_1})\delta(\theta-\theta_{v_0v_1}), \tag{A6}$$

and where the one of the peripheral slot is assumed to be localized on an annular line, namely

$$\frac{1}{\varepsilon}u_2(\theta)=\frac{1}{\varepsilon}U_2(\theta)\frac{1}{r}\,\delta(r-r_2). \tag{A7}$$

Assuming that the particle velocity at the ends of each hole and the slot does not depend on the coordinate over their sections, the behavior of these holes and slot are described by their classical transfer admittances which link the uniform velocity of the flow inside them to the pressure difference between their ends (see details in [1], Eqs. 8a to 10e):

$$u_i = y_i\left[p_C(r_i,\theta)-p(r_i,\theta)\right], \tag{A8}$$

with $y_i=(1-K_{v,i})/(\mathrm{i}\omega\rho_0 h_i)$, where h_i is the length of the orifice, where $K_{v,i}$ accounts for the effect of the viscous boundary layer inside it, and where $p_C(r_i,\theta)$ is the pressure variation in the backchamber.

As mentioned in section 2, the effects inducing additional so-called minor losses [11], namely separation of flow and even formation of vortices, which may appear around the sharp ends of the holes and slots, are neglected because the additional resistance $R_{m\ell}(u_i)$ (y_i being replaced by $1/[R_{m\ell}(u_i)+1/y_i]$) equivalent to these losses is much lower than the resistance of the air gap.

Finally, the pressure field inside the backchamber is assumed to be governed by a propagation equation which presents the same form as equation A3, the values of the parameter which depends on the geometry being different and the sign in the right hand side being opposite (see details in [1]).

The analytical solutions, namely the intricate behavior of the membrane in the large frequency range of interest (up to 100 kHz for a half-inch microphone), are obtained from a method relying on the sets of the appropriate eigenmodes of both the membrane and the pressure fields behind the membrane, and relying partly on the Green's theorem and the associated integral formulation (see details in [1]). Note that the subscript "μ" should be replaced by zero in equation (33.c) in the previous paper [1]: this correction implies that part of the factor in this equation does not depend anymore on the azimuthal coordinate. Therefore, it leads to improve the analytical results presented herein by only partly reducing the azimuthal variations of the displacement field, but it does not modify significantly the values of the amplitudes (which are improved herein). On the other hand, the sensitivity is not modified because it does not depend on the modes $m\neq 0$.

Acknowledgments

The authors would like to express their thanks to Petr Honzík and Jean-Noël Durocher for helpful discussions.

References

[1] T. Lavergne, S. Durand, M. Bruneau, N. Joly, D. Rodrigues: Dynamic behavior of the circular membrane of an electrostatic microphone: Effect of holes in the backing electrode. J. Acoust. Soc. Am. **128** (2010) 3459-3477.

[2] A. J. Zuckerwar: Theoretical response of condenser microphones. J. Acoust. Soc. Am. **64** (1978) 1278-1285.

[3] D. Homentcovschi, R. N. Miles: An analytical-numerical method for determining the mechanical response of a condenser microphone. J. Acoust. Soc. Am. **130** (2011) 3698-3705.

[4] M. J. Herring Jensen, E. S. Olsen: Virtual prototyping of condenser microphones using the finite element method for detailed electric, mechanic, and acoustic characterization. Proceedings of Meetings on Acoustics **19** (2013) 030039.

[5] S. Barrera-Figueroa, K. Rasmussen, F. Jacobsen: The acoustic center of laboratory standard microphones. J. Acoust. Soc. Am. **120** (2006) 2668-2675.

[6] S. Barrera-Figueroa, K. Rasmussen, F. Jacobsen: Hybrid method for determining the parameters of condenser microphones from measured membrane velocities and numerical calculations. J. Acoust. Soc. Am. **126** (2009) 1788-1795.

[7] A. J. Zuckerwar, G. C. Herring, B. R. Elbing: Calibration of the pressure sensitivity of microphones by a free-field method at frequencies up to 80 kHz. J. Acoust. Soc. Am. **119** (2006) 320-329.

[8] D. Rodrigues, C. Guianvarc'h, J.-N. Durocher, M. Bruneau, A.-M. Bruneau: A method to measure and interpret input impedance of small acoustic components. J. Sound Vib. **315** (2008) 890-910.

[9] S. Ollivier, E. Salze, M. Averiyanov, P. Yuldashev, V. Khokhlova, P. Blanc-Benon: Calibration method for high frequency microphones. Acoustics 2012, 11ème Congrès Français d'Acoustique & 2012 Annual IOA (Institute of Acoustics, UK), 13-17 April, Nantes (2012) 3503-3507.

[10] N. Joly: Finite element modeling of thermoviscous acoustics on adapted anisotropic meshes: Implementation of the particle velocity and temperature variation formulation. Acta Acustica united with Acustica **96** (2010) 102-114.

[11] P. J. Morris, S. Boluriaan, C. M. Shieh: Numerical simulation of minor losses due to a sudden contraction and expansion in high amplitude acoustic resonator. Acta Acustica united with Acustica **90** (2004) 393-409.

[12] W. Koidan: Calibration of standard condenser microphones: Coupler versus electrostatic actuator. J. Acoust. Soc. Am. **44** (1968) 1451-1453.